

A CASE OF MESOSCALE CONVECTIVE COMPLEX EVOLVING INTO A VORTEX*

Tao Zuyu (陶祖钰), Wang Hongqing (王洪庆), Bai Jie (白洁)

Laboratory for Severe Storm Research, Department of Geophysics, Peking University, Beijing 100871

Zhu Wenqin (朱文琴), Shi Dingpu (石定朴) and Yang Hongmei (杨红梅)

Institute of Mesoscale Meteorology, Chinese Academy of Meteorological Sciences, Beijing 100081

Received September 1, 1994; revised December 3, 1994

ABSTRACT

A case of mesoscale convective complex (MCC) which evolved into a vortex is documented in this paper. As the MCC entered into the dissipating phase, a well-defined spirally banded structure became visible in the satellite image. The blackbody temperature (TBB) of the residual cold-cloud-shield indicates the vortex existed in the layer from 400 to 250 hPa. According to the upper air analysis, the upper level vortex was an anticyclone. The MCC-generated vortex was visualized in the satellite images because it was located in the subtropical high where the wind field was very weak.

Key words: mesoscale convective complex (MCC), blackbody temperature, mesoscale vortex

1. INTRODUCTION

The upper tropospheric mesoscale anticyclone is one of the principal features of mesoscale convective complex (MCC), which was indicated first by Fritsch and Maddox (1981). But this kind of mesoscale circulation system has not been documented in China, because it is hardly visualized in satellite images. However, in the summer of 1992, we found a distinct MCC-generated vortex in the central China. As shown in the satellite images of Fig. 1, two convective cells in Henan Province merged on the night of the first of August and developed into a typical MCC at 0200 BST (Beijing Summer Time) of August 2. When the MCC was in dissipating phase on the morning of August 2, the well-defined spirally-banded structure of the vortex can be seen distinctly in the enhanced infrared satellite image at 0700 BST of August 2. This paper will describe the evolution of the MCC-generated vortex. The condition of the MCC development will be discussed briefly.

Hourly numerical data of GMS satellite infrared image from 2000 BST of August 1 to 0700 BST of August 4 1992 are used in this study. Due to the fact that the data of the analysis region have been converted to the grid data in Lambert projection, the shape of MCCs can be displayed clearly. The grid size of data is 376×302 with an 8 km horizontal resolution. Then, the grid data of the blackbody temperature (TBB) of cloud top are retrieved from the grey scale (0—255) by use of the curve shown in Fig. 2 after "User Guide of Microcomputer Processing System for GMS", National Satellite Meteorology Center, 1992. Two kinds of charts, the enhanced infrared image and the isoline graph of the cold-cloud-shield temperature, are used to examine the evolution of the MCC.

* This study was supported by the National Natural Science Foundation of China, No. 49335062.

The synoptical environment overview of this case will be given in Section II. The evolution of the MCC is given in Section III by the aid of the hourly TBB isoline graphs of the cold-cloud-shield. Finally, discussions are presented in Section IV.

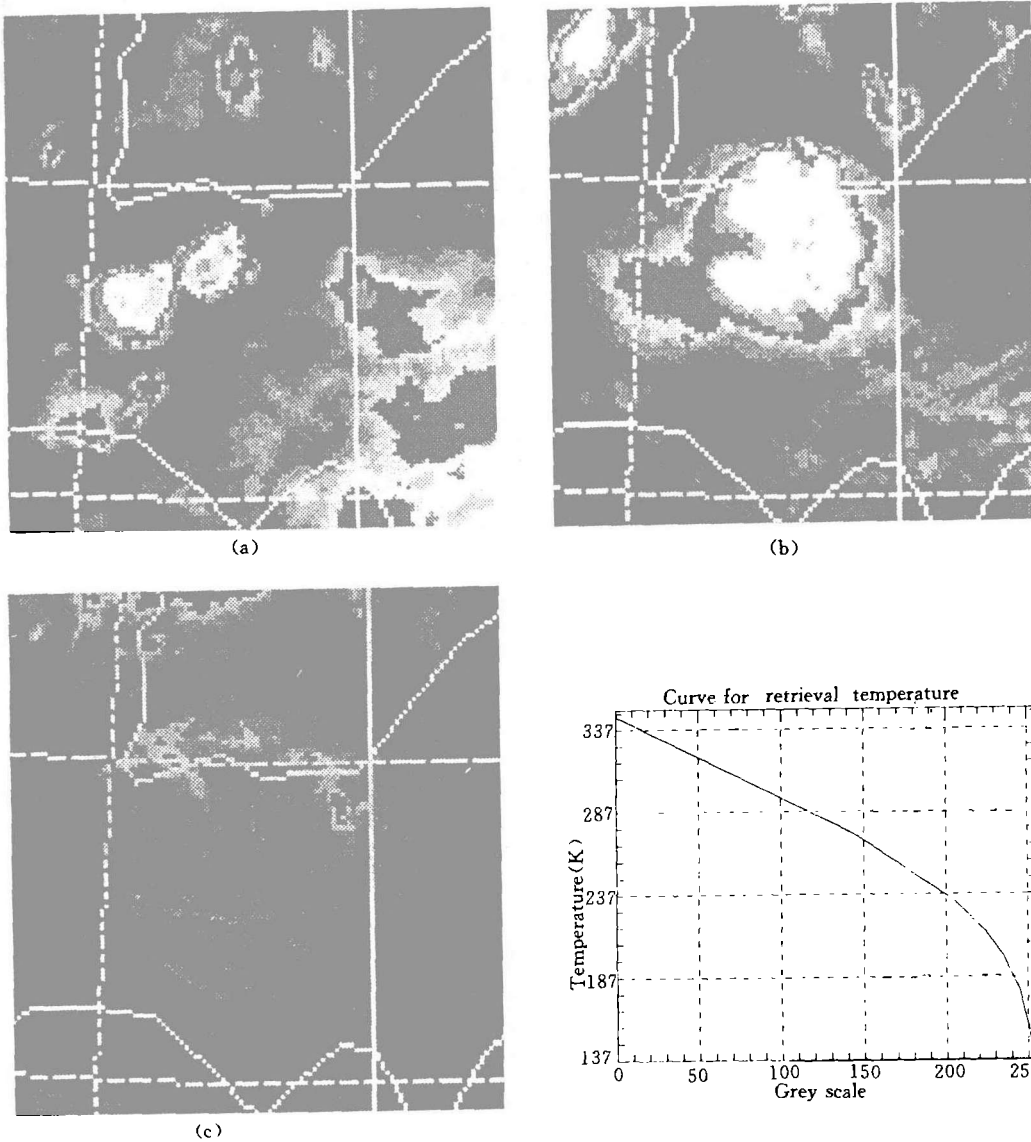


Fig. 1. The detailed enhanced infrared satellite images of the MCC occurring during the night of 1–2 August 1992 in Henan Province of Central China. (a) Initial phase (2200 BST August 1); (b) mature phase (0200 BST August 2); (c) dissipating phase (0700 BST August 2).

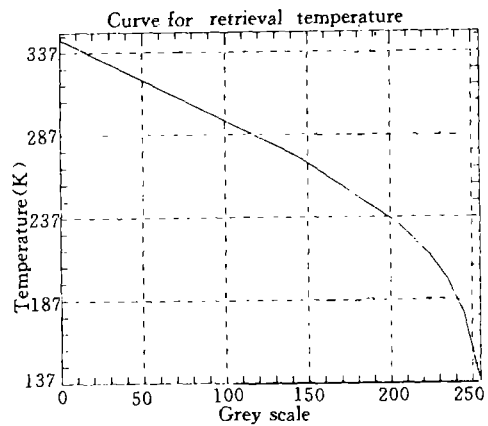


Fig. 2. The blackbody temperatures corresponding to the grey scales from 0–255 of GMS satellite images (taken from "User Guide of Micro-Computer Processing System for GMS", National Satellite Meteorology Center, 1992).

II. CASE OVERVIEW

In 1–4 August 1992, many convection cells occurred in mainland China. Some of them developed into the MCC. From the enhanced infrared satellite image at 0200 BST of August 2 and the 500 hPa analysis at 2000 BST of August 1 given in Fig.3, we can find that a large-scale frontal cloud band extended from Mongolia southward to the Huanghe River. Some MCCs occurred within a couple of hundred kilometers ahead of the front, i.e. Shaanxi, Shanxi, Hebei Provinces of North China and Sichuan Province of Southwest China. But, the structure of those MCCs did not exhibit a clear vortex form. Only the MCC occurring in the 500 hPa subtropical high between the Huanghe River and Changjing River exhibited the vortex form when it entered the dissipating phase. The spirally-banded structure of this MCC became visible in the satellite image, which may be due to that it was located farther away from the frontal region than other MCCs. In the atmosphere with very weak baroclinicity, the shear of winds is so weak that the mesoscale flow pattern associated with the MCC can be distinguished from the large-scale wind field.

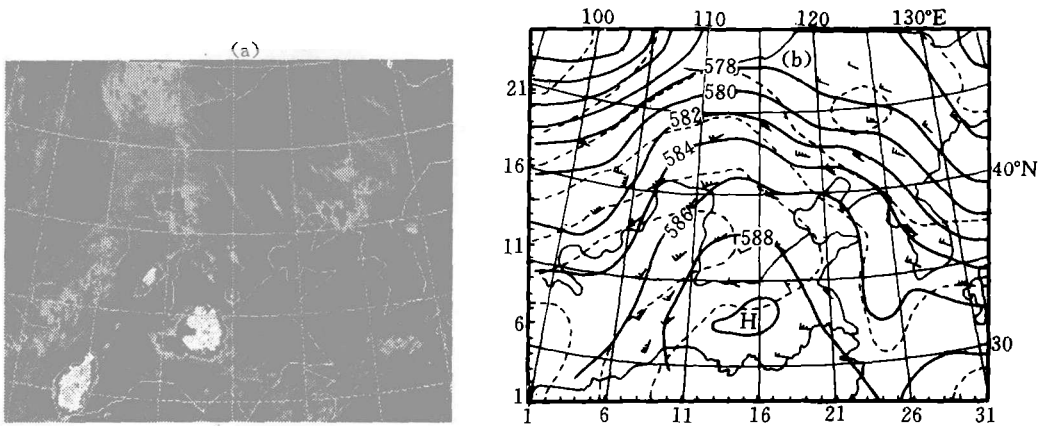


Fig. 3. The enhanced infrared satellite images in Lambert projection at 0300 BST of August 2 1992 (a) and the 500 hPa isobaric analysis at 2000 BST of August 1 1992 (b).

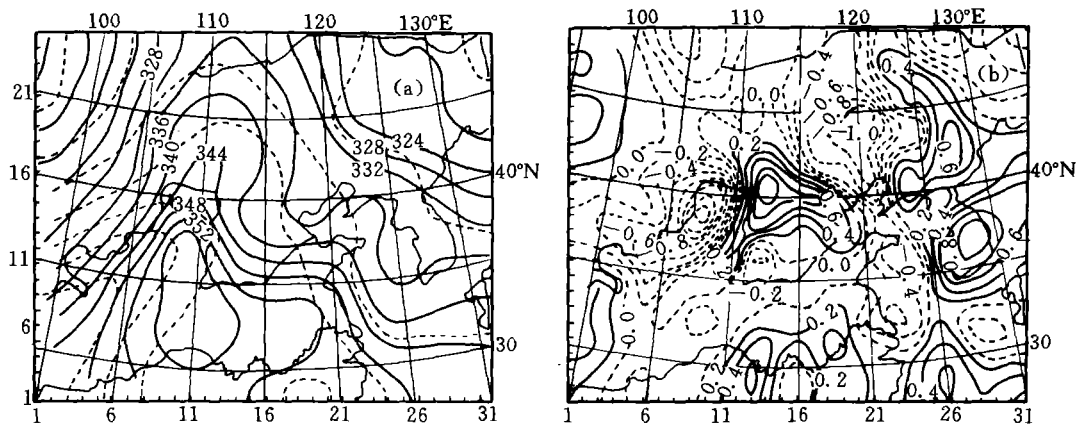


Fig. 4. Equivalent potential temperature and low level flow at 2000 BST of August 1 1992. (a) Isolines of equivalent potential temperature (in unit K; solid: 850 hPa; dashed: 500 hPa); (b) observed winds and isolines of 850 hPa divergence (in unit $10^{-5} s^{-1}$, negative is dashed).

Normally, the convections related to MCC start at 2—3 hours after midday. But in Fig. 1, the convections related to this MCC started at 4—5 hours after the sunset. Therefore, the occurrence of the MCC is not caused by the instability associated with the diurnal circle of the surface temperature. In order to examine the atmospheric instability, the distributions of the equivalent potential temperature θ_e at 850 and 500 hPa are given in Fig. 4a. It can be seen that the low level θ_e is considerably greater than middle level θ_e in the region of the MCC developing. In the Henan Province, the θ_e on 850 hPa is greater than on 500 hPa by over 16 K. It indicates that the MCC developed on the night is due to the stronger convective instability.

In order to explain why this MCC can be developed better in the 500 hPa subtropical high, the observed wind and the divergence fields of 850 hPa are given in Fig. 4b. We can find that this MCC existed in a weaker convergent region between the southerly flow and the easterly flow in the lower layer. Even though the convergence ($-0.4 \times 10^{-5} \text{ s}^{-1}$) in the MCC developing region was much less than the convergence ($-1.4 \times 10^{-5} \text{ s}^{-1}$) associated with the front in the upper reaches of the Huanghe River, resulting weaker ascent could excite the convections in the atmosphere with stronger convective instability and make the MCC formed.

III. EVOLUTION

The TBB isolines of the cloud top are used to examine the evolution of the MCC. According to the definition of the cold-cloud-shield of MCC, the isolines of temperature lower than -30°C are drawn in Fig. 5 for every hour from 2000 BST of August 1 to 0700 BST of August 2. Each block enclosed by dashed lines includes 40×40 grids, and has an area of $102\,400 \text{ km}^2$. Thus, the area of the cold-cloud-shield can be estimated easily.

The origin of the MCC is the convective cells A and B at 2000 BST of August 1 in Fig. 5. Two hours after, these two cells merged, but two separated coldest region ($< -70^\circ\text{C}$) of the cold-cloud-shield could be distinguished. In the following development, the expansion of the cold-cloud-shield was mainly associated with the cell B. The temperature of the cloud top reached the lowest ($< -80^\circ\text{C}$) and the area of the -50°C region expanded to $50\,000 \text{ km}^2$ at 0000 BST of August 2. It indicates that the convection developed into an MCC at this time. In the process of the MCC genesis, there were 5 very small convective cells (indicated by the arrows in Fig. 5) which would be engulfed by the combination of cells A and B. This process may be instrumental to the MCC development.

At 0200 BST, the size of cold-cloud-shield reached the maximum and the area of the temperature lower than -30°C expanded to over $100\,000 \text{ km}^2$. Moreover, the shape of the major part of the MCC (i.e. the cold-cloud-shield associated with cell B) became quasi-circular. After 0200 BST, gradually, the cloud top temperature increased, the cold-cloud-shield broke, and the spirally-banded structure was displayed. It means that the MCC evolved into a vortex at 0700 BST.

Interestingly, the density of the TBB isolines along the border of the convection is related to the tendency of the convection development. It can be seen in Fig. 5 that the convection will be intensified, i.e. the cloud top temperature decreased and the area of cold-cloud-shield expanded, when the TBB isolines are denser along the border. Otherwise, when it becomes thinner, the development will stop and the convection will dissipate. This rule is effective both for small convective cells during the initial phase of MCC and for the MCC in the course of formation to dissipation. It indicates that the TBB analysis of infrared satellite image can be

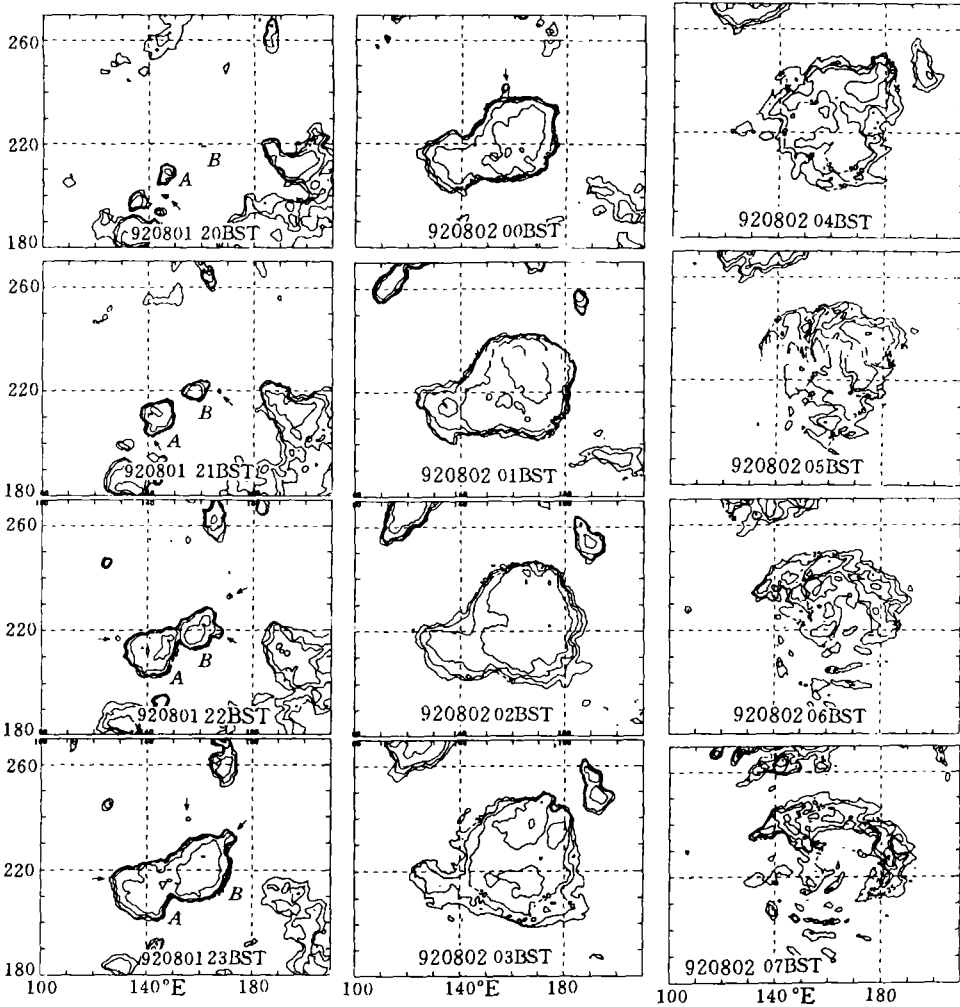


Fig. 5. The TBB isoline graphs of the cold-cloud-shield. The isolines of temperature $< -30^{\circ}\text{C}$ are plotted only. But the maximum is -15 or -25°C for the dissipating phase (0600 and 0700 BST). The interval is 10°C . One block enclosed by the dashed lines includes 40×40 grid points. Its area is about $100\,000\text{ km}^2$. The time is plotted on the graphs.

used not only to examine the structure of the convective system, but also to forecast the convective system.

IV. DISCUSSIONS

The TBB of the residual cold-cloud-shield at 0700 BST 2 August was in the temperature range from -35 to -15°C (see Fig.5), thus the layer where the MCC-generated vortex was located can be estimated to be from 400 to 250 hPa. Figure 6 shows the observed winds and the region with the relative vorticity less than $-4.0 \times 10^{-5}\text{ s}^{-1}$ on 300 hPa at 0800 BST of August 2. It can be seen that the observed winds in the region covered by the MCC exhibit a well-defined anticyclone. The negative vorticity centre of the east side just corresponds to the location of the MCC in Fig. 1c. Consequently, we can say that the spirally-banded structure of the dissipating

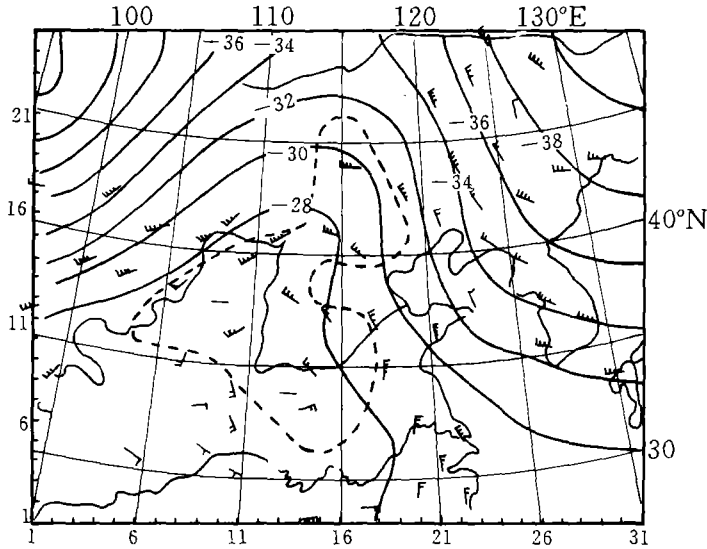


Fig. 6. 300 hPa analysis at 0800 BST of August 2nd 1992 (Solid line is isothermal in unit $^{\circ}\text{C}$. Dashed line is the vorticity contour of $-4 \times 10^{-5} \text{s}^{-1}$. Plotted is the observed winds and temperatures.)

MCC implied an upper-level mesoscale high. The observed temperature plotted in Fig. 6 shows that the 300 hPa temperatures in the area covered by the MCC are higher than -28°C , about 0.5 – 1.0°C warmer than the surrounding areas. It indicates that the 300 hPa mesoscale anticyclone is produced by latent heating which causes the upper isobaric surface rising. Menard and Fritsch (1989) gave a satellite image with a very distinct vortex generated by MCC, but it is a middle-level cyclone. Therefore, the MCC-generated vortex documented in this paper is different from the case given by Menard and Fritsch (1989).

The time series of TBB isoline graphs in Fig. 5 indicate that the centroid of the MCC was stationary, and it was maintained at the initial location of the convective cell B for 12 hours, meaning that the environmental wind field was too weak to shift the MCC. The vortex can be visualized in the satellite images because the circulation of the MCC-generated vortex was not disturbed by the environmental wind.

In summary, the case of an MCC documented in this paper indicates that the upper level mesoscale high is one of the principal forms of a mature MCC. If an MCC occurs in a weaker environmental wind field such as the subtropical high, the vortex structure of the MCC would become visible in the satellite image whenever the MCC enters into the dissipating phase.

I would like to thank Prof. J. M. Fritsch for the discussion of the MCC. Also I would like to thank Mr. Huang Wei for his help about the object analysis.

REFERENCES

- Fritsch, J. M. and Maddox, R. A. (1981), Convectively-driven mesoscale pressure systems aloft, Part I: Observation, *J. Appl. Meteor.* **20**: 9–19.
- Menard, R. D. and Fritsch J. M. (1989), A mesoscale convective complex-generated inertially stable warm core vortex, *Mon. Wea. Rev.*, **117**: 1237–1251.
- National Satellite Meteorology Center (1992), *User guide of micro-computer processing system for GMS*.